Proceedings of the 15th Czech and Slovak Conference on Magnetism, Košice, Slovakia, June 17–21 2013

Magnetoresistance Anisotropy and Magnetic *H*-*T* Phase Diagram of $Tm_{0.996}Yb_{0.004}B_{12}$

N.E. Sluchanko[a,*], A.N. Azarevich[a,b], A.V. Bogach[a], V.V. Glushkov[a,b], S.V. Demishev[a,b], S.Yu. Gavrilkin[c], S. Gabani[d], K. Flachbart[d], N.Yu. Shitsevalova[e], V.B. Filipov[e], J. Vanacken[f], V.V. Moshchalkov[f], J. Stankiewicz[g]

[a]General Physics Institute of RAS, 119991 Moscow, Russia
[b]Moscow Institute of Physics and Technology, 141700 Moscow Region, Russia
[c]Physical Institute of RAS, 53 Leninsky pr.,119991 Moscow, Russia
[d]Institute of Experimental Physics of SAS, 040 01 Košice, Slovak Republic
[e]Institute for Problems of Materials Science NASU, 03680 Kiev, Ukraine
[f]Inst. for Nanoscale Physics and Chemistry, KU Leuven, Leuven 3001, Belgium
[g]Ins. de Ciencia de Materiales de Aragón, Facultad de Ciencias, 50009 Zaragoza, Spain

The antiferromagnetic ground state has been studied by transverse magnetoresistance, heat capacity and magnetization measurements, which were carried out on high quality single crystals of $Tm_{0.996}Yb_{0.004}B_{12}$ dodecaboride in strong magnetic fields at liquid helium temperatures. Both antiferromagnetic-paramagnetic (AF-P) and spin-orientation (AF1-AF2) phase transitions have been observed, and allowed to construct a complicated magnetic *H*-*T* phase diagram for this compound. Strong magnetoresistance anisotropy was found both in AF states ($\rho(H||[110])/\rho(H||[111]) \sim 1.2$ at $H \sim 20$ kOe) and at the critical field of AF-P transition ($H_N[100]/H_N[111] \sim 1.25$) in this magnetic metal with a simple *fcc* crystal structure.

DOI: 10.12693/APhysPolA.126.332

PACS: 72.15.Gd, 73.43.Qt, 75.30.Kz, 75.20.Hr, 75.50.Ee

1. Introduction

It was shown recently that $Tm_{1-x}Yb_xB_{12}$ solid solutions may be considered as model compounds which enable to choose between various scenarios of antiferromagnetic (AF) instability, quantum critical behavior and mechanisms responsible for metal-insulator transition in strongly correlated electron systems [1]. In these conductors with a cage-glass structure [1, 2] the antiferromagnetic state is suppressed and the Neel temperature decreases from $T_N(TmB_{12}) \approx 3.2$ K to $T_N(Tm_{0.74}Yb_{0.26}B_{12})= 0.8$ K during the transition from an AF metal to paramagnetic (P) insulator YbB_{12} with strong electron correlations [3]. In studies [1–3] fast 4*f*-5*d* spin fluctuations were established to be responsible for the formation of heavy fermions and the emergence of spin polarons in the RB_{12} matrix. In this work we investigate the magnetic phase transitions inside the AF state as well as between AF and P phase of $Tm_{0.996}Yb_{0.004}B_{12}$ by transverse magnetoresistance (MR), heat capacity and magnetization measurements. To shed more light on the origin of the complicated AF ground state, we concentrate here on the research of anisotropy both of magnetoresistance and of the magnetic *H*-*T* phase diagram of $Tm_{0.996}Yb_{0.004}B_{12}$.

*corresponding author; e-mail: nes@lt.gpi.ru

2. Experimental details

The single crystals of substitutional $Tm_{1-x}Yb_xB_{12}$ solid solutions were grown by vertical crucible-free induction zone melting in an inert gas atmosphere. Magnetic field, temperature and angular dependences of the transverse magnetoresistance $\Delta\rho/\rho = f(H,T,\phi)$ were measured by dc four-probe method on the unique experimental setup described in [1]. The specific heat of $Tm_{0.996}Yb_{0.004}B_{12}$ single crystals was studied at constant pressure over a wide temperature range 2–300 K in PPMS-9 (Quantum Design), magnetization was investigated by an Oxford Instruments vibrating sample magnetometer (up to 11 T). The quality control of the samples was performed by electron microprobe and X-ray diffraction analysis.

3. Results and discussion

Figure 1 shows $\Delta\rho/\rho = f(H,T_0)$ curves obtained (a) at temperatures 2–4.2 K in the AF and P phases for $\boldsymbol{H}||[110]$ orientation, and (b) at $T = 2.1$ K for $\boldsymbol{H}$ along [110], [100] and [111] axis. The specific features in MR field dependences, indicated by arrows, correspond to both spin orientation (H_M) and AF-P (H_N) phase transitions.

Angular dependences of resistivity presented in Fig. 2 demonstrate directly the anisotropy of MR at $T = 2.1$K in AF and P phases of $Tm_{0.996}Yb_{0.004}B_{12}$. A strong

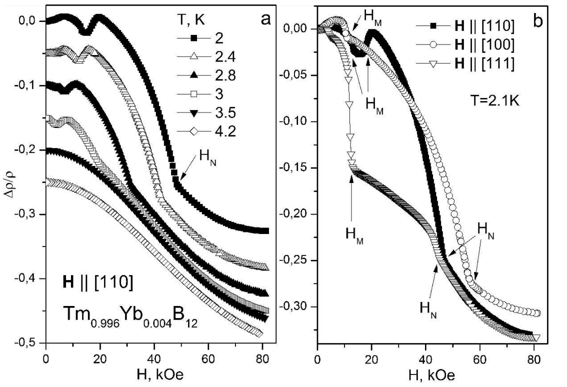

Fig. 1. Magnetic field dependencies of magnetoresistance $\Delta\rho/\rho(H)$ in $Tm_{0.996}Yb_{0.004}B_{12}$ **(a)** at various temperatures in the range 2–4.2 K and for $\boldsymbol{H}||[110]$ (curves are shifted by 0.05 along vertical axis for convenience) and **(b)** at $T = 2.1$ K for three main crystallographic directions. H_N and H_M are critical fields of AF-P and spin-orientation magnetic phase transitions, respectively.

anisotropy of magnetoresistance is observed in the interval 10–40 kOe (Fig. 1b and Fig. 2) and the resistivity ratio $\rho(\boldsymbol{H}||[110])/\rho(\boldsymbol{H}||[111])$ reaches a value of ~ 1.2 in the AF phase at $H \sim 20$ kOe. Additionally, a strong difference between H_N values for $\boldsymbol{H}||[100]$ and $\boldsymbol{H}||[111]$ orientation can be discerned from Fig. 1b ($H_N[100]/H_N[111] \sim 1.25$), pointing to an anisotropy of the AF-P phase boundary in this *fcc* metal. Further, a pronounced hysteresis, both of the angular (see Fig. 2, curves for $H = 10$ kOe) and field dependences of MR, has been found at low magnetic fields $H < 20$ kOe.

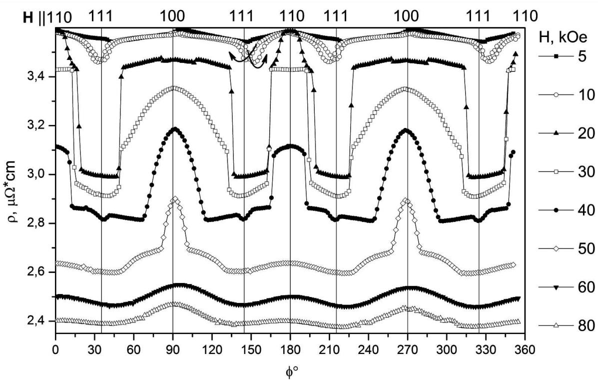

Fig. 2. Angular dependencies of resistivity $\rho(\phi)$ in $Tm_{0.996}Yb_{0.004}B_{12}$ at $T = 2.1$ K for various magnetic fields.

A numerical differentiation of MR field dependences $d(\Delta\rho/\rho)/dH = f(H, T_0)$ (see Fig. 3a) allows to detect precisely the magnetic phase transitions at H_M and H_N and, as a result, to construct in detail the magnetic H-T phase diagram of $Tm_{0.996}Yb_{0.004}B_{12}$ (see Fig. 3b). The undertaken analysis allows to interpret the data in favour of *(i)* an anisotropic character of the AF-P phase boundary (AF2-P in Fig. 3b) and *(ii)* formation of several additional magnetic phases (AF1, AF2 in Fig. 3b) for $\boldsymbol{H}||[110]$ orientation.

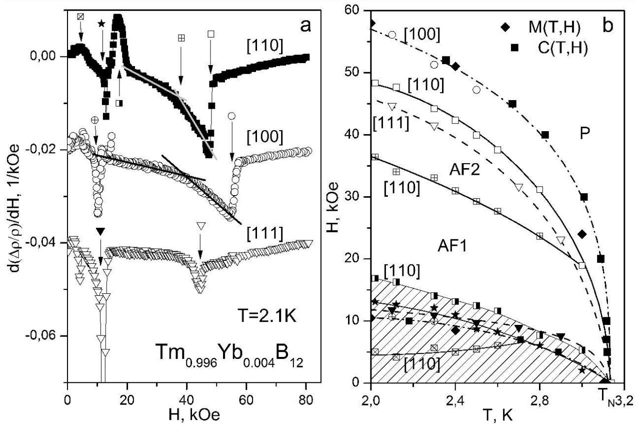

Fig. 3. (a) Derivatives of magnetoresistance $d(\Delta\rho/\rho(H))/dH$ at $T = 2.1$ K for three crystallographic directions (curves are shifted by 0.01 along vertical axis for convenience) and (b) magnetic H-T phase diagram of $Tm_{0.996}Yb_{0.004}B_{12}$. AF1, AF2 are two AF phases, P denotes the paramagnetic phase. Points of phase transitions on panel (a) are shown with arrows and corresponding symbols, the MR hysteresis area is shaded.

4. Conclusions

The magnetoresistance study of $Tm_{0.996}Yb_{0.004}B_{12}$ in AF states and P state allowed to construct the magnetic H-T phase diagram of this antiferromagnet. The anisotropy of both of the AF-P boundaries and the MR behavior at low ($H < 20$ kOe) and intermediate (40–60 kOe) magnetic fields may be interpreted in terms of some additional magnetic interaction, which modifies the magnetic structure produced by RKKY indirect exchange.

Acknowledgments

This work was supported by RAS Program "Strongly Correlated Electrons in Metals, Semiconductors, and Magnetic Materials", Young scientists Grant of RF President No. MK-6427.2014.2, Slovak Scientific Grant Agencies VEGA-2/0106/13, APVV-0132-11 and the Center of Excellence of the Slovak Academy of Sciences.

References

[1] N.E. Sluchanko, A.N. Azarevich, A.V. Bogach, V.V. Glushkov, S.V. Demishev, M.A. Anisimov, A.V. Levchenko, V.B. Filipov, N.Yu. Shitsevalova, *JETP* **115**, 509 (2012).

[2] N.E. Sluchanko, A.N. Azarevich, A.V. Bogach, I.I. Vlasov, V.V. Glushkov, S.V. Demishev, A.A. Maksimov, I.I. Tartakovskii, E.V. Filatov, K. Flachbart, S. Gabani, V.B. Filippov, N.Yu. Shitsevalova, V.V. Moshchalkov, *JETP* **113**, 468 (2011).

[3] F. Iga, N. Shimizu, T. Takabatake, *J. Magn. Magn. Mater.* **177–181**, 337 (1998).